Seroreactivity Against Tyrosine Phosphatase PTPRN Links Type 2 Diabetes and Colorectal Cancer and Identifies a Potential Diagnostic and Therapeutic Target

María Garranzo-Asensio,[1,2] Guillermo Solís-Fernández,[2,3] Ana Montero-Calle,[2] José Manuel García-Martínez,[4] Maria Carmen Fiuza,[5] Pilar Pallares,[6] Nuria Palacios-Garcia,[7] Custodia García-Jiménez,[4] Ana Guzman-Aranguez,[1] and Rodrigo Barderas[2]

Diabetes 2022;71:1–14 | https://doi.org/10.2337/db20-1206

Colorectal cancer(CRC) and diabetes are two of the most prevalent chronic diseases worldwide with dysregulated receptor tyrosine kinase signaling and strong co-occurrence correlation. Plasma autoantibodies represent a promising early diagnostic marker for both diseases before symptoms appear. In this study, we explore the value of autoantibodies against receptor-type tyrosine-protein phosphatase-like N (PTPRN; full-length or selected domains) as diagnostic markers using a cohort of individuals with type 2 diabetes (T2D), CRC, or both diseases or healthy individuals. We show that PTPRN autoantibody levels in plasma discriminated between patients with T2D with and without CRC. Consistently, high PTPRN expression correlated with decreased survival of patients with CRC. Mechanistically, PTPRN depletion significantly reduced invasiveness of CRC cells in vitro and liver homing and metastasis in vivo by means of a dysregulation of the epithelial-mesenchymal transition and a decrease of the insulin receptor signaling pathway. Therefore, PTPRN autoantibodies may represent a particularly helpful marker for the stratification of patients with T2D at high risk of developing CRC. Consistent with the critical role played by tyrosine kinases in diabetes and tumor biology, we provide evidence that tyrosine phosphatases such as PTPRN may hold potential as therapeutic targets in patients with CRC.

Cancer and diabetes are among the most prevalent chronic diseases worldwide. Diabetes encompasses a group of metabolic diseases in which insulin deficiency and/or resistance results in hyperglycemia (1). In type 1 diabetes (T1D), there is an autoimmune destruction of pancreatic β-cells that produces a complete insulin deficiency (1,2). These patients usually have autoantibodies against insulin, GAD65, and tyrosine phosphatase–related proteins such as receptor-type tyrosine-protein phosphatase-like N (PTPRN; more commonly known as islet antigen-2). In contrast, type 2 diabetes (T2D) is characterized by insulin resistance (1). In contrast with T1D, T2D develops slowly during adulthood as a consequence of insulin resistance with initial hyperinsulinemia to compensate. Insulin receptor belongs to the tyrosine kinase (TK) superfamily, and its signaling is altered in both types of diabetes. Constitutively active TK signaling is a hallmark of cancer. TK signaling is switched off by tyrosine-phosphatases, which, not surprisingly, are also frequently altered in cancers. The protein family of phosphotyrosine phosphatase receptors (PTPR), with 21 members, is

[1]Departamento de Bioquímica y Biología Molecular, Facultad de Óptica y Optometría, Universidad Complutense de Madrid, Madrid, Spain
[2]Chronic Disease Programme (UFIEC), Instituto de Salud Carlos III, Madrid, Spain
[3]Molecular Imaging and Photonics Division, Chemistry Department, Faculty of Sciences, KU Leuven, Leuven, Belgium
[4]Area of Physiology, Department of CBS, Faculty of Health Sciences, Rey Juan Carlos University, Madrid, Spain
[5]Surgery Department, University Hospital Fundación Alcorcon, Madrid, Spain
[6]Central Units, Instituto de Salud Carlos III, Madrid, Spain
[7]Endocrinology Department, Hospital Universitario Puerta de Hierro Majadahonda, Madrid, Spain

Corresponding author: Rodrigo Barderas, r.barderasm@isciii.es

Received 28 November 2020 and accepted 13 December 2021
This article contains supplementary material online at https://doi.org/10.2337/figshare.17267837.

M.G.-A., G.S.-F., and A.M.-C. contributed equally to this work.

involved in immune regulation and in vascular and nervous system development (3–6). Although this protein family still remains poorly characterized in cancer, PTPR proteins with oncogenic and tumor suppressor features have been reported in different cancers (7).

PTPRN is a single-pass transmembrane protein found in secretory vesicles and plasma membrane. PTPRN is composed of an extracellular domain (ECD), a single transmembrane region, and an intracellular domain (ICD). Notably, cleaved ICD translocates into the nucleus of β-cells, where it induces the expression of the insulin gene through convergence with STAT3 and STAT5 signaling. In addition, PTPRN, which does not have intrinsic phosphatase activity, might regulate tyrosine phosphatase PTPRA through dimerization (8). Aberrant PTPRN expression has been reported in diabetes and cancer (9,10). PTPRN is expressed in the pancreatic islets and neuroendocrine cells, suggesting that it plays an important role in hormone and neurotransmitter secretion (11–14). In cancer, PTPRN is considered an unfavorable disease marker for hepatocellular carcinoma and glioblastoma (12,15). In addition, PTPRN alterations (mutations, deletions, etc.) have been reported in many cancer types. Furthermore, PTPRN hypermethylation and overexpression correlates with increased tumor growth, cellular proliferation, and shorter survival in ovarian and small cell lung cancer (13,16). However, the importance of PTPRN alterations in highly prevalent cancer types, such as colorectal cancer (CRC), remains unknown.

In T1D, PTPRN is a common target of autoantibodies, for which levels can be measured to detect and predict the pathology (9). In cancer, autoantibodies are commonly produced against tumor-associated antigens well before the clinical symptoms appear (17–21). Therefore, they offer an interesting alternative as disease biomarkers. Thus, cancer-related autoantibodies are usually produced against proteins involved in cancer initiation and/or progression and proteins that modulate the tumorigenic properties of cancer cells (proliferation, invasion, aggressiveness, etc., which could help narrowing down potential disease markers and therapeutic targets) (22). Since patients with T2D have an increased CRC risk (after correction for obesity and other confounding factors) compared with the general population (2,23–25), autoantibodies might serve to identify patients with CRC among individuals with T2D.

In this work, we have analyzed PTPRN seroreactivity in a well-characterized patient cohort composed of healthy individuals, patients with T2D, patients with CRC, and patients with CRC and T2D to determine its usefulness to discriminate patients with CRC. Interestingly, the seroreactivity analysis was able to significantly discriminate control subjects and individuals with diabetes from those with CRC and diabetes, indicating PTPRN seroreactivity could help in the identification of those patients with T2D more prone to develop CRC. Furthermore, PTPRN in vitro and in vivo loss-of-function assays evidenced an important role of PTPRN in the tumorigenic and metastatic properties of CRC cells.

RESEARCH DESIGN AND METHODS

Study Population

Thirty-eight individuals, including patients diagnosed with T2D or/and CRC who underwent surgery at Hospital Fundación Alcorcón (Madrid, Spain) and healthy control subjects, were assessed for eligibility according to the following inclusion/exclusion criteria (Table 1 and Supplementary Table 1). Inclusion criteria were patients who: *1*) underwent surgery to remove visceral fat with T2D, *2*) were the same as in *1*) but without diabetes, *3*) were going to undergo surgery to remove a CRC tumor and have diabetes, or *4*) were the same as *3*) but without diabetes. Recruited patients were divided between the two sexes and had comparable BMI and age. Exclusion criteria were patients who: *1*) consume large amounts of alcohol or are smokers, *2*) have papillomavirus or *Helicobacter pylori* infections, *3*) were treated with immunosuppressants prior to surgery, *4*) were treated with chemotherapy prior to surgery, *5*) who suffer from infectious diseases, *6*) were receiving radiation therapy, or *7*) with autoimmune inflammatory pathology, because these conditions may alter per se the presence of tumor markers in blood. T1

The institutional review board of Hospital Fundación Alcorcón evaluated the clinical and ethical aspects of the study, granting approval on 8 June 2017. All patients gave written informed consent for the use of their biological samples for research purposes. Ethical principles promoted by Spain (LOPD 15/1999) and the European Union Fundamental Rights of the EU (2000/C364/01) were followed. All patients' data were processed according to the Declaration of Helsinki (last revision 2013) and Spanish National Biomedical Research Law (14/2007, of 3 July 2007). Blood samples were rapidly processed to obtain plasma fractions and stored at −80°C until use (19,26–28).

For the evaluation of PTPRN seroreactivity and its ECD and ICD, experiments were performed in triplicate. A total of 18 patients with CRC (10 plasma samples from patients without diabetes with CRC and 8 plasma samples from patients with T2D and CRC) and 20 control samples (10 plasma samples from healthy control individuals and 10 plasma samples from individuals with T2D) were used (Table 1).

Table 1—Plasma samples used for the seroreactivity analysis of PTPRN and its domains

Group	Samples (male/female)	Age (years), median ± SD
Control subjects	4/6	44 ± 11
T2D	7/3	65 ± 12
CRC	6/4	70 ± 12
CRC with T2D	5/3	65 ± 8

Cell Lines

KM12C and KM12SM isogenic CRC cell lines used for the in vitro functional cell-based and in vivo assays were obtained from I. Fidler's laboratory (MD Anderson Cancer Center). KM12SM cells possess high metastatic capacity to liver, whereas KM12C cells are poorly metastatic (29,30). KM12SM cells stably expressing firefly luciferase (KM12SM-vLuc cells) were obtained according to established protocols (31).

Cells were grown and maintained in DMEM supplemented with 10% inactivated FBS, L-glutamine, and penicillin/streptomycin at 37°C and 5% CO_2. Every 15 days, cells were monitored for the absence of mycoplasma contamination.

Gateway Plasmid Construction, Gene Cloning, DNA Preparation, and Protein Expression

Sequence-verified, full-length cDNA plasmid containing PTPRN, ECD, and ICD of PTPRN and HaloTag protein were obtained either from the publicly available DNASU Plasmid Repository (https://dnasu.org/DNASU/) or by PCR using specific primers (Supplementary Table 2 and Supplementary Material) (32–34).

SDS-PAGE and Western Blot Analysis

SDS-PAGE and Western blot (WB) analysis to assess protein quality were performed as previously reported (34,35). Briefly, 0.67 μL of the in vitro protein extracts or 10 μg of KM12C and KM12SM protein extracts were separated in 10% SDS-PAGE and transferred to nitrocellulose membranes (Hybond-C Extra). After blocking, membranes were incubated overnight at 4°C with an anti-HaloTag monoclonal antibody (#6921A; Promega) diluted 1:1,000, an anti-PTPRN monoclonal antibody (sc-130570; Santa Cruz Biotechnology) diluted 1:200, an anti–phosphorylated (p-)insulin Rβ polyclonal antibody (sc-25103-R; Santa Cruz Biotechnology) diluted 1:1,000, an anti-IRS1 polyclonal antibody (sc-559; Santa Cruz Biotechnology) diluted 1:1,000, an anti–p-FOXO1/3 polyclonal antibody (#9464; Cell Signaling Technology), an anti-AKT polyclonal antibody (#4691; Cell Signaling Technology,), an anti–p-AKT polyclonal antibody (#9275; Cell Signaling Technology), an anti-ERK polyclonal antibody (#4695; Cell Signaling Technology), an anti–p-ERK polyclonal antibody (#9101; Cell Signaling Technology), an anti-GSK3β monoclonal antibody (#61021; BD Transduction Laboratories,), an anti-GAPDH (800–656–7625; Rockland Immunochemicals) diluted 1:2,000, or an anti-RhoGDi (sc-360; Santa Cruz Biotechnology) diluted 1:1,000. Immunodetection on nitrocellulose membranes was achieved by using horseradish peroxidase–conjugated goat anti-mouse IgG antibody or horseradish peroxidase–conjugated goat anti-rabbit IgG antibody (Sigma-Aldrich). Chemiluminescence signal was developed with ECL Western Blotting Substrate (Thermo Fisher Scientific) and detected on an Amersham Imager 680 (GE Healthcare).

Bioinformatic Analysis

Meta-analysis information regarding PTPRN genetic and protein expression levels in CRC was retrieved from the cBioPortal (https://www.cbioportal.org/) and Oncomine (https://www.oncomine.org/). Survival analyses were performed using the GEPIA2 web server (https://gepia2.cancer-pku.cn/#index), and colon adenocarcinoma (COAD) and/or rectal adenocarcinoma (READ) The Cancer Genome Atlas (TCGA) data sets.

Epstein-Barr Antigen 1 ELISA and PTPRN Luminescence Beads Seroreactive Immunoassay

Colorimetric ELISA for Epstein-Barr antigen 1 (EBNA1) antibody determination for the evaluation of the specificity of the study was achieved coating 0.05 μg of EBNA1 protein (kindly provided by Protein Alternatives, SL) per well in 50 μL of PBS solution in 96-well transparent plates (Nunc) overnight at 4°C according to established protocols (32,34,36).

PTPRN luminescence bead seroreactive immunoassay was performed according to established protocols (32,34). See Supplementary Material for information in detail.

Transient PTPRN Silencing

For transient PTPRN silencing, transfection was performed in six-well plates using the jetPRIME reactive (PolyPlus Transfection) with, alternatively, three siRNAs targeting PTPRN to account for potential off-target effect (PTPRN #1, SIHP0814-SIHP0816, Sigma-Aldrich; PTPRN #2, EHU029231, Sigma-Aldrich; and PTPRN #3, sc-62902, Santa Cruz Biotechnology) or control siRNAs (SIC001; Sigma-Aldrich) following the manufacturer's instructions. Briefly, 2.5×10^5 cells were transfected with 55 pmol siRNA using 2 μL of jetPRIME Transfection reagent and 50 μL of jetPRIME buffer. Then, 48 h after transfection, cells were analyzed by semiquantitative PCR or WB.

RNA Extraction, cDNA Synthesis, Semiquantitative PCR, and Real-time Quantitative PCR

RNA was extracted from cell lines using TRIzol reagent (Sigma-Aldrich) and the RNeasy Mini Kit (Qiagen) according to the manufacturer's instructions. The RNA was quantified using a NanoDrop ND-1000 spectrophotometer (NanoDrop Technologies Inc.) and used for cDNA synthesis using the NZY First-Strand cDNA Synthesis Kit (NZYTech). cDNA was used for semiquantitative PCR using PTPRN-specific primers to evaluate gene silencing (Supplementary Table 2). Alternatively, cDNA was used for semiquantitative PCR (two replicates) and/or quantitative PCR (qPCR) (two replicates in duplicate) analyses upon transient PTPRN depletion of: *1*) dysregulation of epithelial-mesenchymal transition (EMT) markers using specific primers of transforming growth factor-β1 (TGF-β1), Snail1 (SNAI1 gene), Claudin-2, E-cadherin (CDH1), *N*-cadherin (CDH2), and ZO1 (TJP1 gene); and *2*) the analysis of the insulin receptor signaling pathway using specific

primers of mTOR, FOXO1, AS160, ERK1, ERK2, IRS1, AKT1, AKT2, and GSK3α (Supplementary Table 2). 18S was used as internal loading control. Semiquantitative PCR reactions were performed using the Phusion High-Fidelity DNA Polymerase (Thermo Fisher Scientific). For qPCR, reactions were performed using TB-Green Premix Ex Taq (Tli RNase H Plus; Takara Bio), and PCR and data collection were performed on a Light Cycler 480 (Roche). All quantitations were normalized using human 18S.

Invasion, Proliferation, and Wound Healing Assays

Invasion, proliferation and wound healing assays were performed in duplicate as previously described (37). See Supplementary Material for detailed information.

In Vivo Animal Experiments

The Ethical Committee of the Instituto de Salud Carlos III (Spain) approved the protocols used for experimental work with mice after approval for the ethical committee OEBA (Proex 285/19). For liver homing analysis, Nude mice were intrasplenically inoculated with 1×10^6 KM12SM cells after 24 h of transient transfection with PTPRN ($n = 1$/siRNA) or control ($n = 2$) siRNAs in 0.1 mL PBS. Mice were euthanized 24 h after intrasplenical cell inoculation and RNA from liver and spleen isolated using TRIzol reagent. RNA was analyzed by RT-PCR to amplify human GAPDH and murine β-actin as loading control using specific primers (Supplementary Table 2). For metastasis experiments, 1×10^6 KM12SM-vLuc liver metastatic CRC cells after 24 h of transient transfection with PTPRN or control siRNAs was intrasplenically injected in Nude mice (Charles River Laboratories) in 0.1 mL PBS. The spleen was resected the day after, and then mice were inspected daily. Two weeks after intrasplenical cell inoculation, liver metastases were quantified in isoflurane-anesthetized mice by luminescent activity of KM12SM-vLuc cells using luciferin (12.5 mg/kg, intraperitoneal injection). Luminescence was recorded with the IVIS in vivo imaging system (PerkinElmer) every 7 days up to 60 days after intrasplenical cell injection. At day 60, mice were sacrificed and inspected visually and by luminescence for the presence of liver metastasis.

Statistical Analysis

Data are presented as mean ± SD. All statistical analyses were performed with Microsoft Office Excel and the R program (version 3.6.1). For the analysis of the seroreactivity assays, the evaluation of the statistical significance between groups was performed using the *t* test, and *P* values <0.05 were considered statistically significant. Parametric test (*t* test) was used taking into account that our sample size was large enough (>30), without outliers, and with the mean of the data of the groups mostly representing the center of the distribution of the data. The diagnostic ability of PTPRN and ECD and ICD was evaluated by receiver operating characteristic (ROC) curves. ROC curves, their corresponding area under the curve (AUC), and maximized sensitivity and specificity values were calculated using the R package Epi (38).

For the analysis of the in vitro assays and qPCR data, the evaluation of the statistical significance between groups was performed using the *t* test, and *P* values <0.05 were considered statistically significant.

Data and Resource Availability

All data generated or analyzed during this study are included in this published article or available upon request.

RESULTS

Since patients with T2D are at higher risk than patients without diabetes to develop CRC (2,24), we hypothesized that PTPRN could be dysregulated in CRC and molecularly associated to the co-occurrence of cancer in patients with T2D.

Meta-Analysis of PTPRN in CRC

First, the potential alteration of PTPRN in CRC was evaluated by meta-analysis using public databases. The examination of the Oncomine database revealed higher mRNA expression of PTPRN in CRC compared with normal tissue (Fig. 1*A*) (39,40). The examination of the TCGA cohort related to COAD and READ revealed PTPRN mutations in ∼3% of patients with CRC (Fig. 1*B*). Seven mutations leading to the loss of phosphatase function were found. Lastly, the COAD and READ TCGA data sets were used for PTPRN-associated survival analysis assessed by Kaplan-Meier curves using the median for separating high and low PTPRN expression. The significance of the difference in survival between both populations was estimated by the log-rank test. An inverse association between PTPRN expression and overall or disease-free survival of COAD and CRC was revealed (*P* values <0.05) (Fig. 1*C*). For overall survival analysis, only 40% of patients with CRC with high PTPRN expression levels survived ∼6 years. In contrast, 75% of patients with CRC with low PTPRN expression levels survived ≥6 years. Moreover, for disease-free survival analysis, 40% of patients with CRC with high PTPRN expression levels showed no recurrence after 6 years of diagnosis in comparison with the 65% of patients with CRC showing low PTPRN expression levels. F1

Collectively, these data show that PTPRN alterations are present in CRC, with high PTPRN expression associated with a worse prognosis, indicating that PTPRN expression levels could be used as a malignant prognostic factor in the disease.

In Vitro Expression of PTPRN and Evaluation of its Humoral Immune Response

Then, since protein alterations have been associated to the development of humoral immune responses in patients with cancer (41,42), the ability of PTPRN to induce a

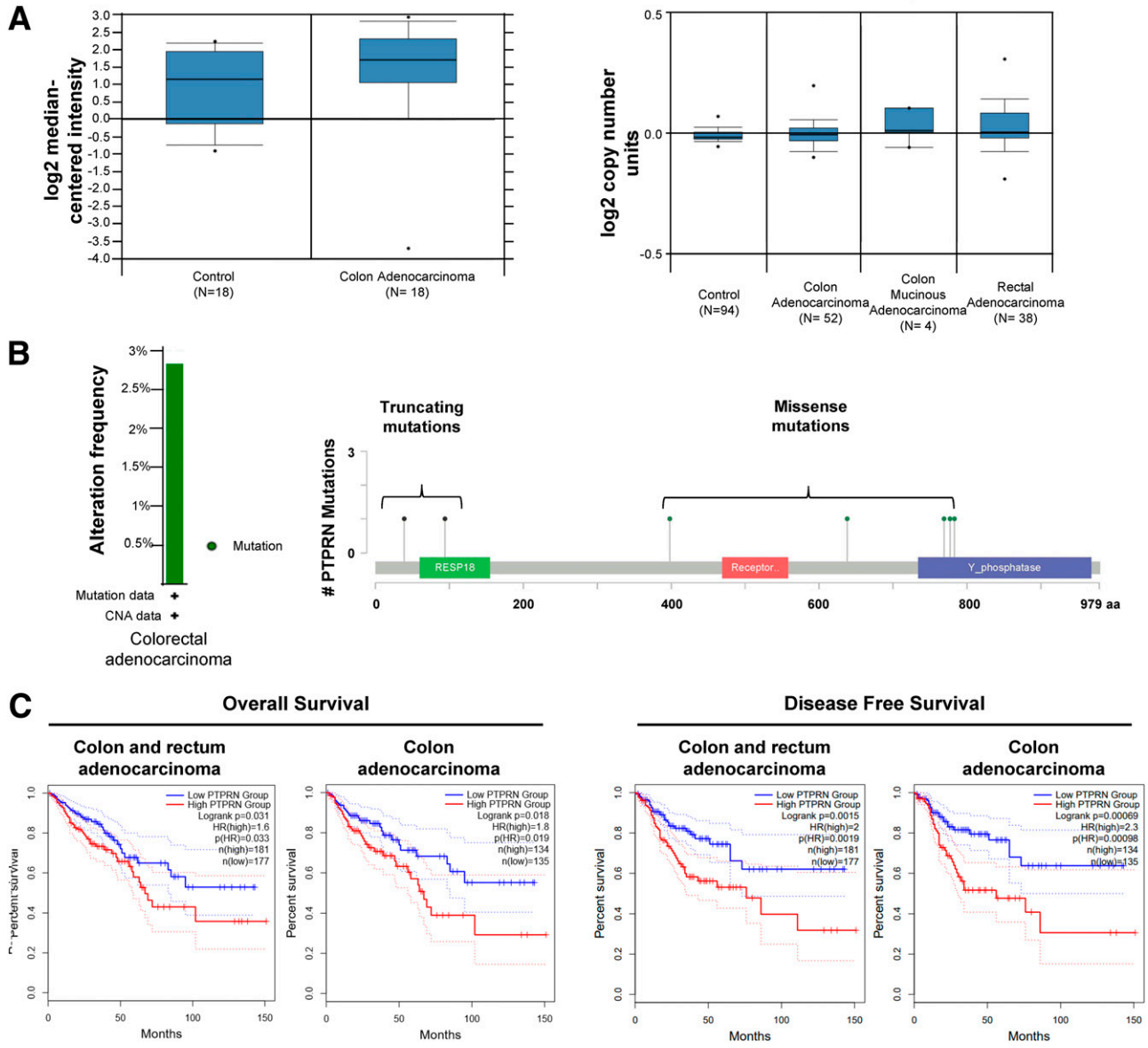

Figure 1—Assessment of PTPRN dysregulation in CRC. *A:* Evaluation of mRNA levels in CRC tissue compared with normal adjacent tissue using Oncomine. Higher PTPRN mRNA levels were found in CRC tissue in comparison with control tissue (39,40). *B*: The cBioPortal database retrieved data about the presence of PTPRN mutations at a genetic level in ∼3% of patients with CRC (TCGA, COAD). *C*: Survival analysis retrieved from the GEPIA2 web-based tool revealed that a higher PTPRN expression in patients with CRC (READ and COAD) and patients with COAD (TCGA data sets) was related with a large decrease in their overall and disease-free survival (P values < 0.05). CNA, copy number alteration; HR, hazard ratio.

humoral immune response in patients with CRC was evaluated. Given that PTPRN is recognized by autoantibodies of patients with T1D, we also evaluated if the population with T2D, which has an increased CRC risk, presents PTPRN autoantibodies.

To this end, we produced the protein in vitro and measured the specific immunoreactivity present in the plasma of patients with T2D or CRC or both compared with healthy subjects. Full-length PTPRN, as well as its ICD and ECD (Fig. 2*A*), were expressed fused to HaloTag in the C-terminal end using an in vitro cell-free expression system (33,34,36). HaloTag allows purifying the fusion proteins by covalent immobilization with magnetic beads (MBs) for direct evaluation of autoantibody levels in plasma samples.

Fusion proteins were correctly expressed (Fig. 2*B*) and immobilized onto the MBs (Fig. 2*C*) with no degradation that could interfere in the screening as shown by immunostaining. HaloTag functionality was verified by incubation of the fusion proteins with chloroalkane functionalized MBs that covalently bound HaloTag and an antibody specific against the tag. Signal was developed in all cases,

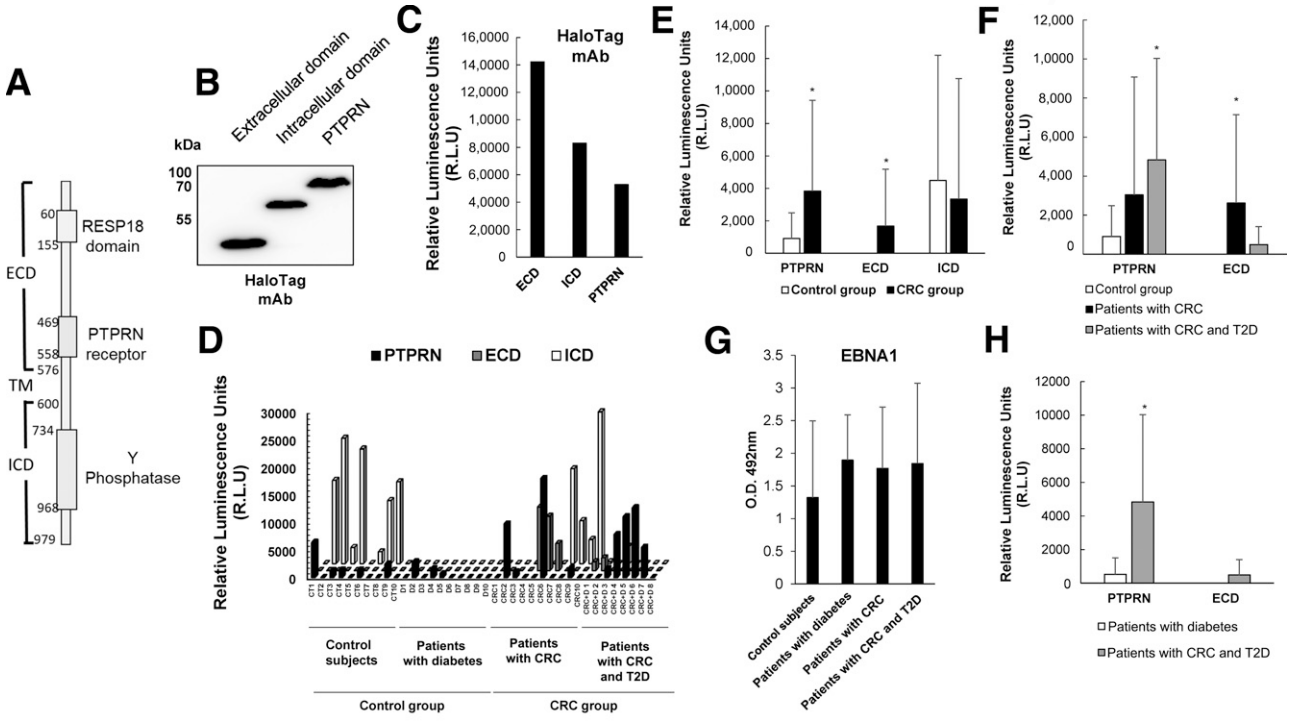

Figure 2—In vitro PTPRN expression and seroreactivity analysis of PTPRN. *A*: PTPRN (979 aa in length) is composed of a signal peptide (SP), an ECD, a transmembrane domain (TM), and an ICD. The amino acids composing each domain are highlighted. *B*: Immunostaining using a monoclonal antibody against the HaloTag of the indicated fusion proteins in vitro expressed. *C*: Covalent immobilization of the proteins into MBs by HaloTag was verified through luminescence using a monoclonal antibody against the tag. *D*: Seroreactivity analysis of autoantibodies against ECD, ICD, and PTPRN in plasma samples from healthy individuals and those with diabetes, CRC, and CRC with T2D. *E*: PTPRN and ECD seroreactivity was significantly higher in the CRC group than in the control group (*P* value <0.05). *F*: When comparing the control group with the patients with CRC and the CRC with patients with T2D separately, PTPRN could significantly discriminate between control subjects and patients with T2D with CRC (*P* value <0.05), whereas ECD could significantly discriminate between the control group and the patients with CRC (*P* value <0.05). *G*: Not statistically significant differences were found when comparing EBNA1 seroreactivity among groups. EBNA1 seroreactivity was used as control because $>90\%$ of the human population has antibodies against EBNA1. *H*: Both PTPRN and ECD autoantibodies could discriminate between individuals with diabetes and patients with CRC and patients with CRC with T2D separately (*P* values <0.05). Measurements were performed in triplicate. Bar graphs represent the mean ± SD (*E*, *F*, and *H*). $*P < 0.05$.

indicating that the tag (fused to the proteins) was successfully attached into the MB surface (Fig. 2*C*).

Once established the optimal working conditions, we evaluated whether PTPRN or its domains could discriminate between patients with CRC, T2D, or T2D with CRC or healthy individuals (Fig. 2*D*). To this end, plasma samples were separately evaluated for the control groups (healthy people and individuals with T2D) versus the CRC group (with or without T2D). When the seroreactivity of samples from patients with T2D with or without CRC was evaluated against the fusion proteins, both PTPRN full-length and ECD were able to discriminate patients with CRC from control subjects ($P < 0.03$) (Fig. 2*E*), whereas ICD showed no discrimination potential and similar high background or unspecific signal in both groups. PTPRN and ECD seroreactivity were higher in patients with CRC or with T2D and CRC as compared with the control group (Fig. 2*F*). However, only full-length PTPRN could significantly discriminate between control subjects and patients with T2D with CRC. In contrast, only ECD could discriminate with statistical significance between the control group and patients with CRC (Fig. 2*F*). The data suggest that the seroreactivity present in patients with CRC is mainly directed toward ECD. As control of the specificity of the assay, seroreactivity toward EBNA1 was evaluated in parallel. No significant differences (*P* values >0.1) were found among all groups (Fig. 2*G*).

Finally, comparison of the seroreactivity of patients with T2D with and without CRC revealed that full-length PTPRN discriminated with statistical significance the presence/absence of CRC in patients with T2D (Fig. 2*H*). Therefore, PTPRN appeared as a useful blood-based biomarker to discriminate CRC in patients with T2D.

Diagnostic Ability of PTPRN in Patients With CRC

Lastly, to evaluate the diagnostic potential of the detection of autoantibodies, we obtained ROC curves. When discriminating control and CRC groups using autoantibodies against PTPRN (full-length and ECD), an overall AUC

of 76.5% (sensitivity 55.6% and specificity 95.0%) was found, suggesting their potential for the detection of the pathology (Fig. 3*A*). Furthermore, an overall AUC of 90.0% (sensitivity 75.0% and specificity 100%) was found to discriminate patients with T2D with CRC from those without. The results indicate the usefulness of PTPRN full-length and ECD autoantibodies to screen patients with T2D with a potential risk of developing CRC (Fig. 3*B*).

PTPRN Depletion Reduces the Tumorigenic Properties of CRC Cell Lines

To understand how PTPRN influences the tumorigenic properties of CRC, we used two isogenic CRC cell lines with opposite metastatic properties. Liver metastatic KM12SM cells show the highest levels of PTPRN expression (Fig. 4*A*) in contrast to nonmetastatic KM12C cells.

PTPRN transient silencing followed by invasion, proliferation, and wound healing assays was used in KM12C and KM12SM cells compared with scrambled cells to assess PTPRN influence in tumorigenic and metastatic properties. First, depletion of PTPRN by transient silencing using three different siRNAs was efficiently achieved as observed by PCR and WB analyses (Fig. 4*B*). Next, tumorigenic and metastatic properties were assessed.

Using Matrigel invasion assays, PTPRN-depleted KM12C and KM12SM CRC cell lines exhibited reduced invasiveness as compared with scrambled control cells using the three independent PTPRN siRNAs (P values <0.05) (Fig. 4*C*). Next, in proliferation assays, PTPRN-depleted KM12C and KM12SM cells proliferated less with PTPRN siRNAs #1 and #3 than control cells transfected with the scrambled siRNA (P values <0.05) (Fig. 4*D*). Consistent with their origin and different metastatic properties, there were more KM12SM cells capable of invading the Transwell chamber through the Matrigel than KM12C cells. In addition, KM12SM cells showed higher proliferation rates than nonmetastatic primary tumor KM12C cells.

Since invasion appeared to be more affected than proliferation by PTPRN silencing, wound healing assays were used to confirm a role of PTPRN on cell migration using PTPRN siRNA #1 (Fig. 4*E*). KM12SM cells tend to close the wound faster than KM12C. Both PTPRN-silenced cell lines closed the wound at a slower rate than their control cells transfected with the scramble siRNA with a significantly higher effect on KM12SM cells (Fig. 4*E*), for which PTPRN expression was higher (Fig. 4*A*). The speed of migration was calculated for both conditions. The primary control cells, KM12C cells transfected with scrambled siRNA, migrated at an average speed of 102 ± 5 pixels/h, while KM12C cells transfected with PTPRN siRNA migrated at an average speed of 71 ± 28 pixels/h, indicating a 30% reduction in the migration speed after PTPRN depletion. Likewise, the average migration speed was decreased in the metastatic KM12SM cells upon PTPRN depletion. Consistent with their origin, the average migration speed of the metastatic KM12SM cells was higher than that of KM12C cells, and it decreased from values of 140 ± 82 pixels/h to 109 ± 34 pixels/h for the cells transiently transfected with scrambled and PTPRN siRNAs, respectively.

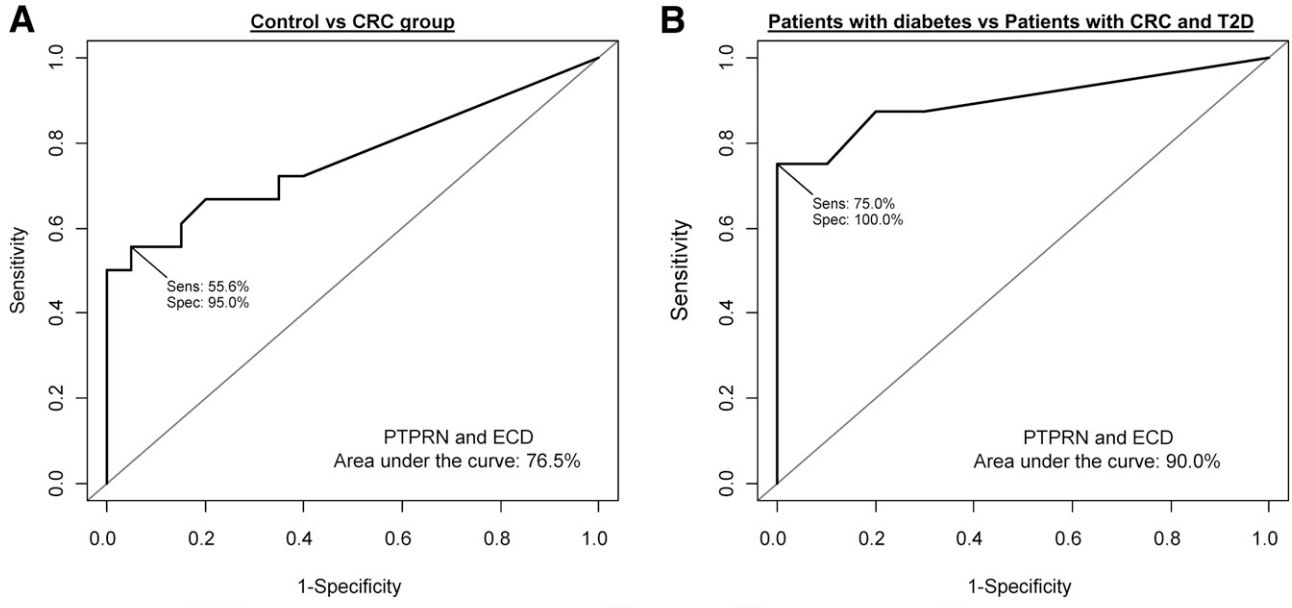

Figure 3—Diagnostic potential of the detection of PTPRN autoantibodies. The diagnostic potential for the detection of autoantibodies against PTPRN and ECD was evaluated using ROC curves. *A*: Autoantibody detection could discriminate between control and CRC group with an AUC of 75.5%. *B*: Autoantibody detection could discriminate between patients with T2D and CRC with patients with T2D with an AUC of 90.0%. Sens, sensitivy; Spec, specificity.

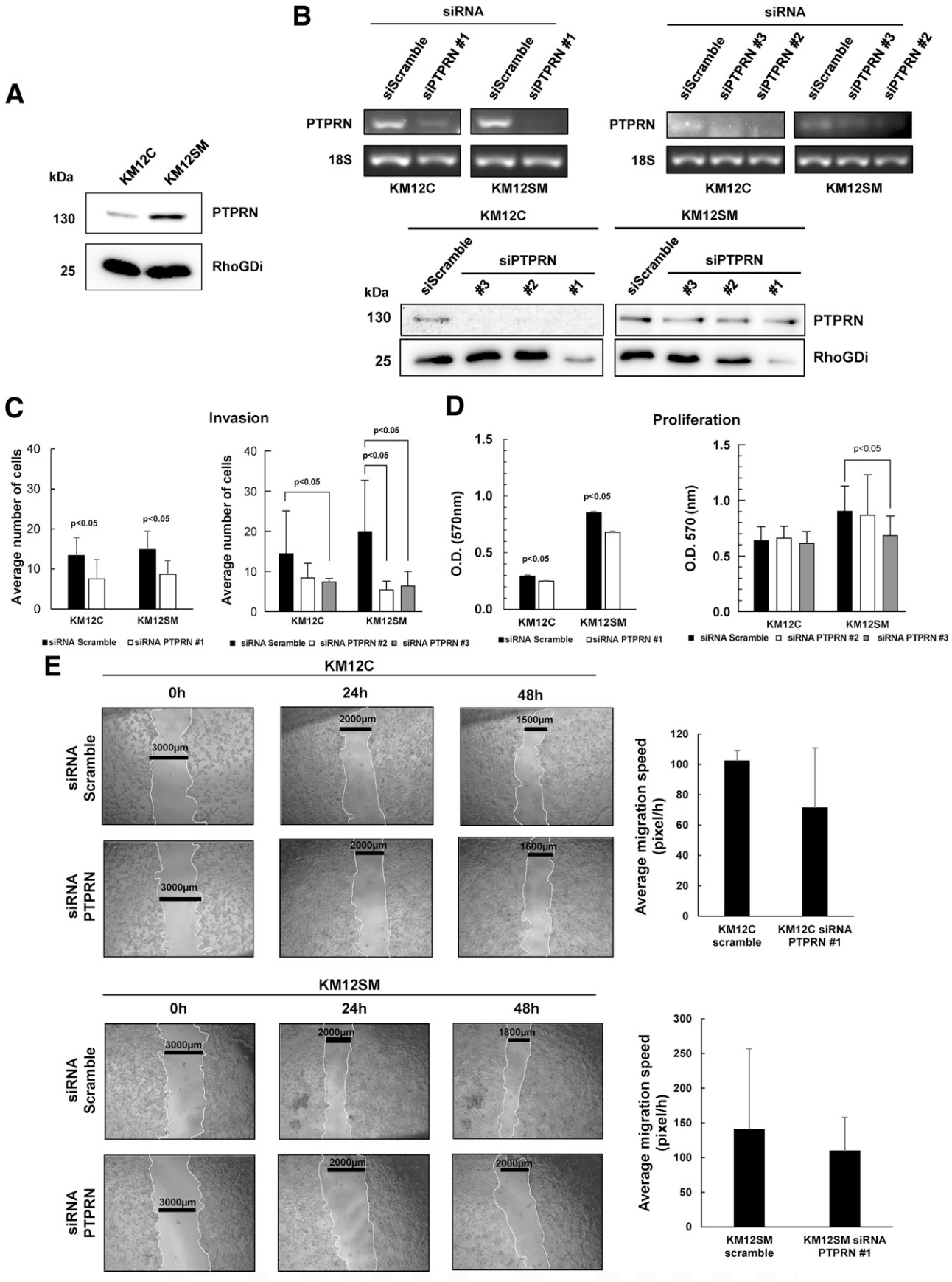

Figure 4—Silencing of PTPRN in KM12C and KM12SM CRC cells and effect on their tumorigenic properties. *A*: Protein expression levels in CRC cell lines KM12C and KM12SM. RhoGDi was used as loading control. *B*: Evaluation by PCR and WB of the transient silencing of

PTPRN Silencing on Metastatic CRC Cell Lines Reduces the Expression of Inducers of the Mesenchymal Phenotype

EMT of epithelial cells is associated to malignancy and supports changes in cell proliferation, migration, and invasion, which were reduced by PTPRN depletion in our assays. Therefore, we investigated whether PTPRN depletion alters EMT inducers in CRC cells (Fig. 5*A* and *B*). F5

Changes in the mRNA expression levels of TGF-β1, Snail1 (SNAI1 gene), Claudin-2, E-cadherin (CDH1), *N*-cadherin (CDH2), and ZO1 (TJP1 gene) were analyzed by semiquantitative PCR (Fig. 5*A*) and qPCR (Fig. 5*B*) analyses. PTPRN depletion caused in both KM12C and KM12SM cells a significant decrease in EMT inducers TGF-β1 and SNAI1. Moreover, a slight dysregulation of tight junctions' proteins ZO1 and Claudin-2 suggested that PTPRN depletion provokes at least a partial reversion of the EMT transition. Differences were more pronounced in KM12SM highly metastatic CRC cells to liver than in KM12C cells, where the decrease in the EMT inducers SNAI1 and TGF-β1 was surprisingly not accompanied by an increase in the epithelial marker E-cadherin and a decrease of *N*-cadherin. Although quantitative results corroborated the dysregulation of EMT markers observed by semiquantitative PCR analyses, further studies are needed to understand whether these proteins are further regulated posttranscriptionally.

PTPRN Depletion Alters the Insulin Receptor Signaling Pathway

We next explored whether PTPRN depletion in isogenic nonmetastatic and metastatic CRC cells could also affect insulin receptor signaling, as a surrogate marker of the interrelationship of PTPRN between T2D and cancer. To this end, the expression levels of insulin receptor and insulin receptor signaling intermediates were explored by PCR, qPCR, and/or WB (Fig. 5*C* and *D*).

A decrease in the mRNA expression levels of IRS1, GSK3α, FOXO1, mTOR, AS160, AKT1, AKT2, ERK1, and ERK2 was observed upon PTPRN depletion in both KM12C and KM12SM cells by semiquantitative PCR and/or qPCR analyses (Fig. 5*C* and *D*), showing that PTPRN depletion impact insulin receptor signaling by altering the basal levels of its intermediate molecules. Again, quantitative results, which showed a similar alteration in IR signaling with the three siRNAs, corroborated observations at semiquantitative level. WB for IRS1, AKT, and ERK confirmed previous results on mRNA (Fig. 5*E*). In addition, as observed by WB, PTPRN depletion decreased precursor and mature p-IRβ, p-AKT, p-ERK, and p-FOXO1/3 protein levels in KM12C and KM12SM cells. On the contrary, GSK3β at protein level was overexpressed upon PTPRN depletion.

Collectively, albeit certain variability attributable to the use of three independent siRNAs, data suggest that PTPRN depletion alters insulin receptor signaling. This alteration, in turn contributes to the dysregulation of the EMT, leading to a partial reduction of the EMT process with the subsequent diminished proliferation, migration, and invasion observed in CRC cells.

PTPRN Depletion Decreases Liver Metastasis Ability of CRC Cells

In vivo effects of the transiently PTPRN depletion was investigated on KM12SM CRC liver metastatic cells. First, KM12SM cells were inoculated in the spleen of nude mice to examine PTPRN effects on the capacity for liver homing. As a surrogate marker for homing, human GAPDH was barely detected in the livers of mice inoculated with transiently transfected siRNAs #1 and #2 against PTPRN or decreased (#3) in comparison with KM12SM cells transfected with scramble (Fig. 6*A*). F6

Therefore, as PTPRN seems to be important for liver homing and metastatic colonization in CRC, we further studied the role of PTPRN on metastasis formation and growth. After intrasplenic inoculation of KM12SM-vLuc cells transiently transfected with siRNAs 24 h prior to inoculation, luciferase expression was assessed as a proxy of liver metastatic growth every 7 days from day 20 to day 60, when control mice started showing distress signs (Fig. 6*B*). Interestingly, PTPRN depleted cells upon intrasplenical injection developed significantly lower or nondetectable liver metastatic foci in comparison with control cells (Fig. 6*B* and *C*). Finally, livers from all animals were further visualized by luminescence (Fig. 6*D*). Liver metastatic foci were present in the two control mice. In contrast, only one out of six mice inoculated with PTPRN depleted cells developed substantially smaller metastatic foci. Reduced metastatic formation and growth were associated with the lower capacity for liver colonization of PTPRN-depleted cells. These results suggest that PTPRN is required in CRC cells for liver metastasis in vivo.

PTPRN after 48 h posttransfection using three different siRNAs in KM12C and KM12SM cell lines. As control, we transfected the cell lines with a scrambled siRNA. By PCR, 18S was used as internal control. By WB, RhoGDi was used as loading control. *C* and *D*: PTPRN plays a role in the tumorigenic properties of metastatic CRC cell lines. KM12C and KM12SM transiently transfected with PTPRN siRNAs #1, #2, and #3 showed lower invasion capacity than control (scrambled transfected) cell lines (P values <0.05). *D*: Both KM12C and KM12SM cell lines transiently transfected with PTPRN siRNAs #1 and #3 proliferate at a lower rate than control cells (P values <0.05). *E*: Wound healing assays carried out during 48 h demonstrated that both cell lines migrated at a slower speed when PTPRN was depleted with PTPRN siRNA #1. In agreement with their metastatic properties, KM12SM cells showed higher invasion, proliferation, and migration speed than KM12C cells. All experiments were performed in duplicate. Experiments performed with PTPRN siRNA #1 and siRNAs #2 and #3 were performed separately.

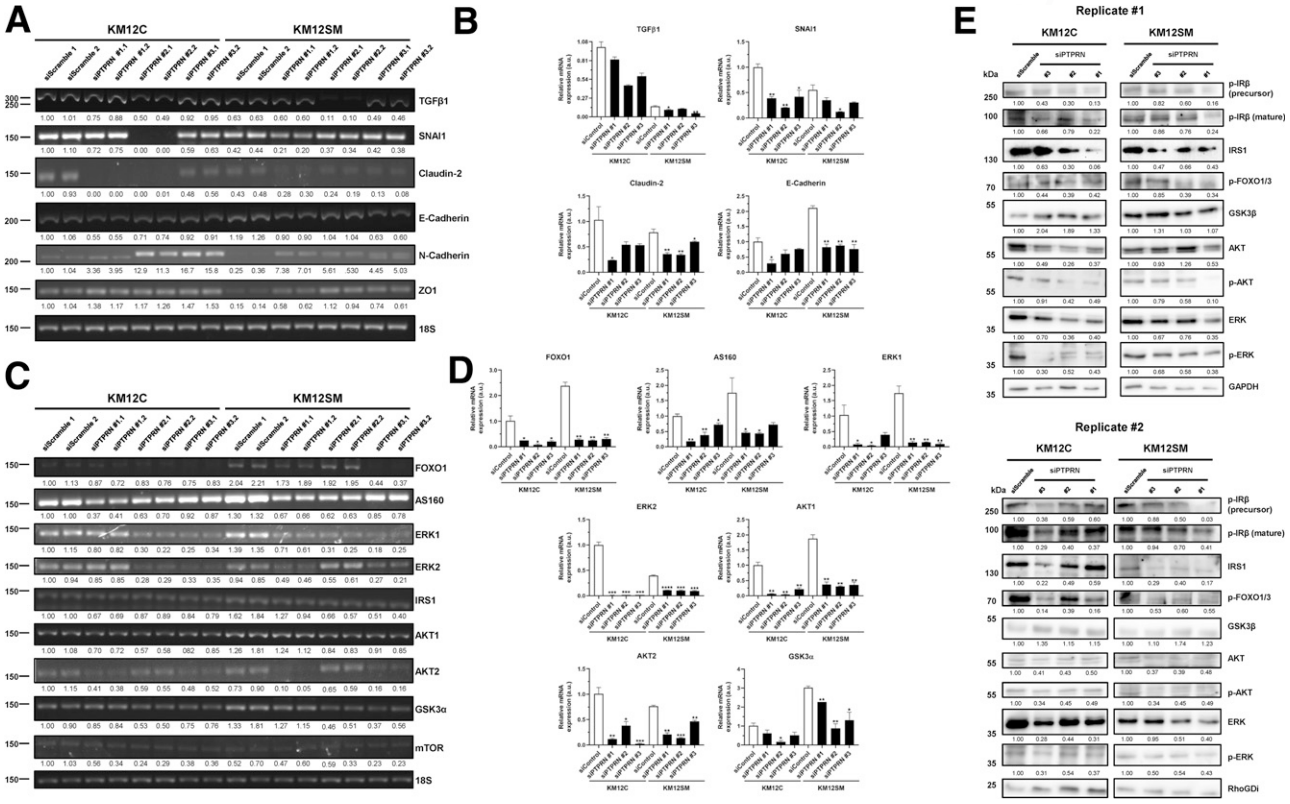

Figure 5—PTPRN depletion on KM12C and KM12SM CRC cells alters EMT transition and reduces insulin receptor signaling pathway. *A* and *B*: Alterations in EMT inducers after PTPRN depletion in KM12C and KM12SM cell lines. cDNA synthesized from total RNA from transiently depleted PTPRN and scrambled control cells was subjected to semiquantitative RT-PCR analysis using specific primers for the EMT inducers TGF-β1, SNAI1, Claudin-2, E-cadherin, *N*-cadherin, and ZO1 using 18S as control and for normalization (*A*) or qPCR analysis using specific primers for TGF-β1, SNAI1, Claudin-2, and E-cadherin using 18S for normalization (*B*). *C–E*: Analysis of alterations in the insulin receptor signaling pathway by PCR and WB, respectively, after PTPRN depletion in KM12C and KM12SM cell lines. cDNA synthesized from total RNA from transiently depleted PTPRN and scrambled control cells after 48 h posttransfection was subjected to semiquantitative RT-PCR analysis using specific primers for IRS1, ERK1, ERK2, AKT1, AKT2, mTOR, FOXO1, AS160, and GSK3α using 18S as control and for normalization (*C*) or qPCR analysis using specific primers for ERK1, ERK2, AKT1, AKT2, mTOR, FOXO1, and GSK3α using 18S for normalization (*D*). *E:* Protein expression levels of p-FOXO1/3, GSK3β, p-IRβ, AKT, p-AKT, ERK, p-ERK, and IRS1 in CRC cell lines KM12C and KM12SM transiently transfected with indicated siRNAs for 48 h confirmed RT-PCR and/or qPCR results. GAPDH and RhoGDi were used as controls. Red Ponceau staining of each line was used for normalization. *A*, *C*, and *E:* Two replicate experiments (#1 and #2) were analyzed. Representative images are shown. *B* and *D:* Data represent the mean ± SD of two experiments. The abundance of each mRNA and protein was quantified by densitometry using ImageJ. a.u., arbitrary units.

DISCUSSION

Dysregulated signaling pathways and specifically signaling by TKs is a hallmark of many cancers and metabolic diseases, such as diabetes, which have been extensively studied. In contrast, the role of tyrosine-phosphatases (including PTPRN), which may play an important role in the tumorigenic process as signaling inactivators, remains unclear (43), although some tyrosine phosphatase receptor alterations were observed in cancer (7). Tyrosine phosphatases dephosphorylate tyrosine residues and have a potential to regulate physiological processes relevant in cancer development as cell proliferation, differentiation, adhesion, and migration. Therefore, cellular homeostasis requires tight regulation of tyrosine phosphatases, and their dysregulation may contribute to the development of diseases. As such, numerous genetic and epigenetic alterations have been described for PTPR receptors, including amplification, deletion, and mutations in PTPRN (43).

Increasing evidence reveals a relationship between diabetes and many cancers (2). Several epidemiologic studies have found that patients with diabetes are at increased risk of developing CRC compared with individuals without diabetes (2,44,45). This relationship is especially relevant in patients with T2D, a disease that develops slowly with early symptoms being frequently silent until diagnosis. Since PTPRN is a well-established diabetes autoantibody, albeit for patients with T1D, and since autoantibodies have been shown to be useful for cancer diagnosis (41), we studied in this work whether the presence of PTPRN autoantibodies might represent another link between diabetes and CRC.

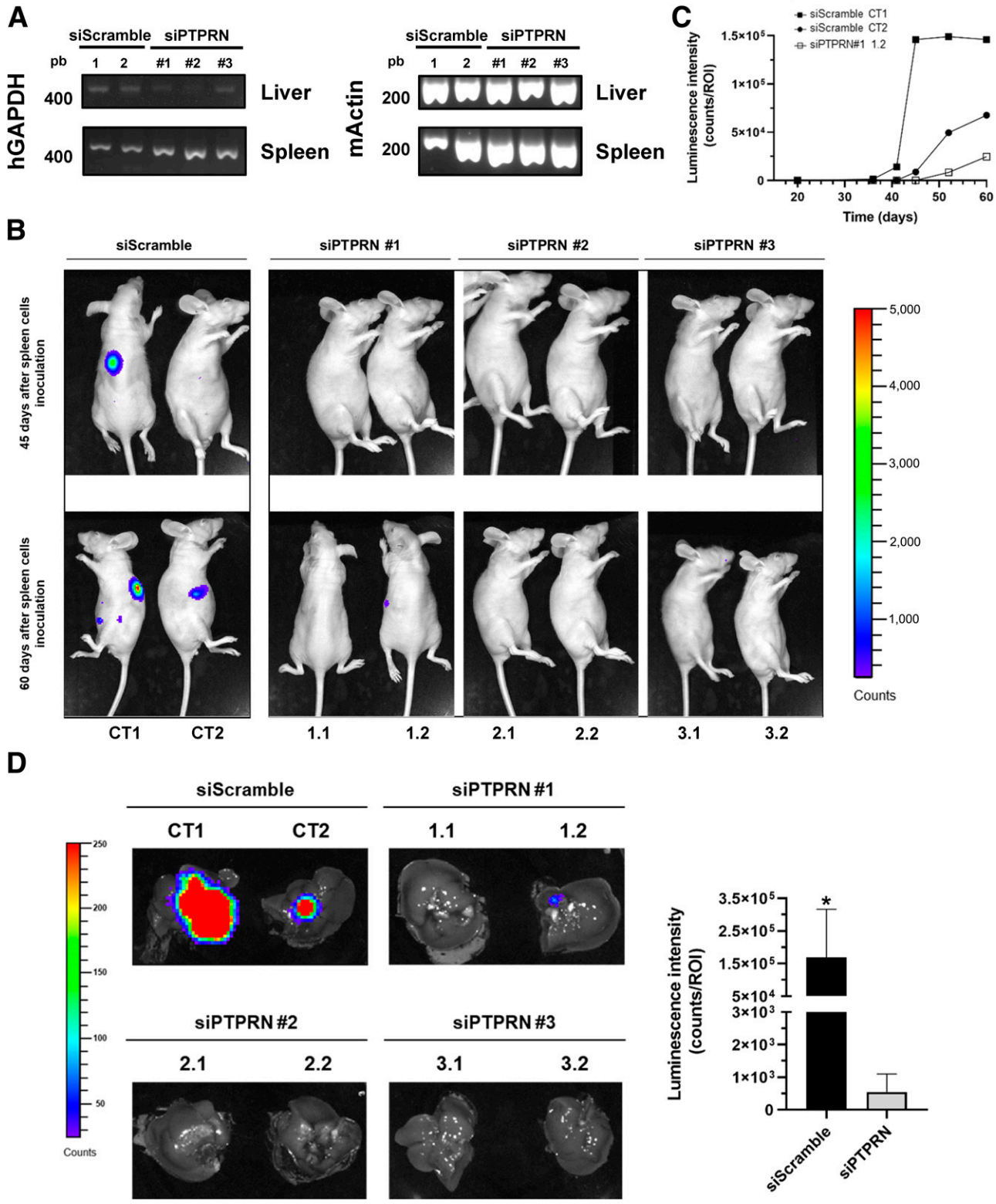

Figure 6—PTPRN depletion decreases liver homing and liver metastasis in KM12SM CRC cells. *A:* Nude mice intrasplenically inoculated with KM12SM cells transiently transfected with siScramble (n = 2) and indicated PTPRN siRNAs (n = 1/PTPRN siRNA) were sacrificed 24 h after inoculation for analysis of in vivo liver homing. RNA was isolated from the liver and spleen (as control) and directly subjected to RT-PCR to amplify human GAPDH (hGAPDH). Representative experiments out of two are shown. Murine β-actin (mActin) was amplified as control. *B:* Representative images of luminescence intensity of in vivo luciferase activity from mice injected with KM12SM cells transiently transfected with control and PTPRN siRNAs at days 45 and 60 postintrasplenical inoculation. Mice injected with control cells did show detectable bioluminescence by IVIS analyses, in contrast to mice injected with PTPRN-depleted cells (one out of six mice showed

Therefore, we have evaluated the potential implication of PTPRN in CRC and T2D. Overall, a direct association between seroreactivity toward PTPRN in patients with CRC and malignancy was observed. Surprisingly, PTPRN autoantibody levels in plasma were a good discriminator between patients with and without CRC for patients without diabetes and even better for patients with T2D. Moreover, since ICD seroreactivity was observed at a similar extent for control subjects and patients with CRC, ECD seemed to be the domain of the protein that induced such response. In addition, patients with CRC with and without T2D showed increased levels of autoantibodies against PTPRN and ECD when compared individually to the control group. ROC curves with the data gathered for the control subjects and CRC group showed an overall AUC of 76.5%, indicating the usefulness of PTPRN as CRC diagnostic autoantibody marker. When comparing the diagnostic potential of autoantibodies to PTPRN and ECD in patients with T2D with and without CRC, an AUC of 90% was achieved. Remarkably, the data suggest that PTPRN and ECD autoantibodies could be used to evaluate the risk of CRC in patients with T2D. To our knowledge, this is the first study linking diabetes and cancer by means of seroreactive analysis of autoantibodies. Given the increased risk of CRC for patients with T2D, our results may translate into preventive strategies on the management of patients with T2D.

Through functional in vitro cell-based assays and in vivo assays, it was made evident that PTPRN silencing produced a shift on the tumorigenic and metastatic properties of the studied colon cancer cell lines. KM12C and KM12SM cell lines lost invasion, proliferation, and migration abilities upon PTPRN depletion. In vivo, PTPRN depletion led to a loss in liver homing and metastatic ability of KM12SM cells. These results suggest that PTPRN plays a role along the progression of CRC, in both primary tumor (KM12C cells) and in metastasis (KM12SM cells). In this sense, and considering the relationship between tumorigenic properties of cancer cells and EMT, the expression of EMT effectors after PTPRN transient depletion reflected a dysregulation on the expression of Snail1, TGF-β1, E-cadherin, and *N*-cadherin, among other EMT effectors and transcription factors that may account for the observed partial reversion of the EMT. Surprisingly, the downregulation of TGF-β1 and Snail1was not accompanied by the opposite upregulation and downregulation of E-cadherin and *N*-cadherin, respectively. This could be associated to the powerful features of EMT transcription factors and their relevance for cancer pathogenesis (46–48), from tumor initiation, establishment of precursor lesions, accumulation of genetic alterations, escape from tumor surveillance, and therapy resistance to the development of metastasis (48,49). These processes provoke a continuous flux between epithelial and mesenchymal end point states (47,48), which is often partially executed (46). Indeed, it has been described a rebound effect in some EMT effectors (i.e., Slug and Snail [50]) (46), which could be associated to this unexpected feature and to a partial EMT dysregulation. Further studies using stably transfected cell lines are needed to elucidate the interactor proteins of PTPRN and its effectors and to understand in detail how PTPRN contributes to the EMT process. However, present data suggest that PTPRN may represent an interesting therapeutic target for CRC and for metastatic CRC to liver. Finally, it is also noteworthy that PTPRN depletion causes also a decrease in the insulin receptor signaling, and in ERK and AKT, that might also explain the changes observed in the expression of EMT genes and the decrease in proliferation, migration, and invasion of CRC cells in vitro, respectively. Noticeably, the decrease on ERK and AKT mRNA and protein levels could be associated with: *1*) the dysregulation of the insulin receptor signaling, *2*) a decrease in PTPRN signaling for which depletion decreased proliferation, invasion, and migration of CRC cells, processes in which AKT and ERK are implicated (43), or *3*) synergistic effects on the dysregulation of both signaling routes. These results further support a role for PTPRN as a link between cancer and diabetes.

Notably, although higher patient samples and multicentric cohorts together with other added factors, such as hyperinsulinemia, should be analyzed in subsequent studies to get further evidence of the role of PTPRN in cancer and diabetes and to overcome some limitations in the study as the number of samples, we have demonstrated in this study a significant relationship between PTPRN, T2D, and CRC progression. These results demonstrate a new link between these highly prevalent chronic diseases. Moreover, in vitro and in vivo assays using stably transfected CRC cells will help to evaluate the mechanisms of action of PTPRN on EMT transition and on ERK and AKT and insulin receptor signaling pathways. Future studies on PTPRN dysregulation in patients with CRC with and without T2D are guaranteed to shed light on its potential for screening patients T2D for CRC. Additionally, PTPRN

detectable luminescence signal). Three mice per group were inoculated, but one mouse of each group died prior to metastasis development because of other causes (i.e., after spleen resection or hemorrhage), and thus, $n = 2$ was the final mice number per group at day 60. *C:* Luminescence per indicated mice was represented at each time points. *D:* At day 60 postintrasplenical cell inoculation, livers from all control or PTPRN siRNA-treated mice were collected and luminescence measured in an IVIS in vivo imaging system. As depicted in the images, one out of six PTPRN siRNA-treated mice showed detectable luminescence, in contrast to the highly measurable luminescence of the two control siRNA mice. Significant luminescence values were observed comparing control and PTPRN siRNA groups, for which luminescence signal was represented by bar graph. ROI, region of interest.*$P < 0.05$.

may offer a new potential therapeutic target in CRC in a clinical setting.

Acknowledgments. The authors thank the excellent technical support of MariCruz Sánchez-Martínez.

Funding. This work was supported by the Ramon y Cajal programme of the MINECO and the financial support of the PI17CIII/00045 and PI20CIII/00019 grants partially supported by FEDER funds from the AES-ISCIII program to R.B. and Mineco/FEDER SAF2016-79837-R and PID2019-110998RB-I00 to C.G.-J. M.G.-A. was supported by a contract of the Programa Operativo de Empleo Juvenil y la Iniciativa de Empleo Juvenil with the participation of the Consejería de Educación, Juventud y Deporte de la Comunidad de Madrid y del Fondo Social Europeo. The FPU predoctoral contract to A.M.-C. is supported by the Spanish Ministerio de Educación, Cultura y Deporte. G.S.-F. is recipient of a predoctoral contract supported by the Flanders Research Foundation (grant no. 1193818N).

Q:3 **Duality of Interest.** No potential conflicts of interest relevant to this article were reported.

Author Contributions. All authors meet the requirements for authorship. M.G.-A., G.S.-F., A.M.-C., J.M.G.-M., M.C.F., P.P., N.P.-G., and A.G.-A. performed the experiments. C.G.-J., A.G.-A., and R.B. designed the experiments. M.G.-A., G.S.-F., A.M.-C., C.G.-J., A.G.-A., and R.B. analyzed the data and wrote the manuscript. M.G.-A. and R.B. are the guarantors of this work and, as such, had full access to all of the data in the study and take responsibility for the integrity of the data and the accuracy of the data analysis.

References

1. American Diabetes Association. Diagnosis and classification of diabetes mellitus. Diabetes Care 2013;36(Suppl. 1):S67–S74

2. García-Jiménez C, Gutiérrez-Salmerón M, Chocarro-Calvo A, García-Martinez JM, Castaño A, De la Vieja A. From obesity to diabetes and cancer: epidemiological links and role of therapies. Br J Cancer 2016;114:716–722

3. Alonso A, Sasin J, Bottini N, et al. Protein tyrosine phosphatases in the human genome. Cell 2004;117:699–711

4. Johnson KG, Van Vactor D. Receptor protein tyrosine phosphatases in nervous system development. Physiol Rev 2003;83:1–24

5. Hendriks WJ, Elson A, Harroch S, Stoker AW. Protein tyrosine phosphatases: functional inferences from mouse models and human diseases. FEBS J 2008;275:816–830

6. Stoker A. Methods for identifying extracellular ligands of RPTPs. Methods 2005;35:80–89

7. Julien SG, Dubé N, Hardy S, Tremblay ML. Inside the human cancer tyrosine phosphatome. Nat Rev Cancer 2011;11:35–49

8. Harashima S, Horiuchi T, Wang Y, Notkins AL, Seino Y, Inagaki N. Sorting nexin 19 regulates the number of dense core vesicles in pancreatic β-cells. J Diabetes Investig 2012;3:52–61

9. Lampasona V, Bearzatto M, Genovese S, Bosi E, Ferrari M, Bonifacio E. Autoantibodies in insulin-dependent diabetes recognize distinct cytoplasmic domains of the protein tyrosine phosphatase-like IA-2 autoantigen. J Immunol 1996;157:2707–2711

10. Xie H, Notkins AL, Lan MS. IA-2, a transmembrane protein tyrosine phosphatase, is expressed in human lung cancer cell lines with neuroendocrine phenotype. Cancer Res 1996;56:2742–2744

11. Notkins AL, Lan MS, Leslie RD. IA-2 and IA-2beta: the immune response in IDDM. Diabetes Metab Rev 1998;14:85–93

12. Zhangyuan G, Yin Y, Zhang W, et al. Prognostic value of phosphotyrosine phosphatases in hepatocellular carcinoma. Cell Physiol Biochem 2018;46:2335–2346

13. Yin W, Tang G, Zhou Q, et al. Expression profile analysis identifies a novel five-gene signature to improve prognosis prediction of glioblastoma. Front Genet 2019;10:419

14. Xu H, Cai T, Carmona GN, Abuhatzira L, Notkins AL. Small cell lung cancer growth is inhibited by miR-342 through its effect of the target gene IA-2. J Transl Med 2016;14:278

15. Shergalis A, Bankhead A 3rd, Luesakul U, Muangsin N, Neamati N. Current challenges and opportunities in treating glioblastoma. Pharmacol Rev 2018;70:412–445

16. Bauerschlag DO, Ammerpohl O, Bräutigam K, et al. Progression-free survival in ovarian cancer is reflected in epigenetic DNA methylation profiles. Oncology 2011;80:12–20

17. Nesterova M, Johnson N, Cheadle C, Cho-Chung YS. Autoantibody biomarker opens a new gateway for cancer diagnosis. Biochim Biophys Acta 2006;1762:398–403

18. Noaki R, Kawahara H, Watanabe K, Ushigome T, Kobayashi S, Yanaga K. Serum p53 antibody is a useful tumor marker of early colorectal cancer. Int Surg 2010;95:287–292

19. Barderas R, Villar-Vázquez R, Fernández-Aceñero MJ, et al. Sporadic colon cancer murine models demonstrate the value of autoantibody detection for preclinical cancer diagnosis. Sci Rep 2013;3:2938

20. Pedersen JW, Gentry-Maharaj A, Fourkala EO, et al. Early detection of cancer in the general population: a blinded case-control study of p53 autoantibodies in colorectal cancer. Br J Cancer 2013;108:107–114

21. Qiu J, Choi G, Li L, et al. Occurrence of autoantibodies to annexin I, 14-3-3 theta and LAMR1 in prediagnostic lung cancer sera. J Clin Oncol 2008; 26:5060–5066

22. Dudas SP, Chatterjee M, Tainsky MA. Usage of cancer associated autoantibodies in the detection of disease. Cancer Biomark 2010;6:257–270

23. Yao C, Nash GF, Hickish T. Management of colorectal cancer and diabetes. J R Soc Med 2014;107:103–109

24. Gutiérrez-Salmerón M, Chocarro-Calvo A, García-Martínez JM, de la Vieja A, García-Jiménez C. Epidemiological bases and molecular mechanisms linking obesity, diabetes, and cancer. Endocrinol Diabetes Nutr 2017;64: 109–117

25. Gutiérrez-Salmerón M, Lucena SR, Chocarro-Calvo A, García-Martínez JM, Martín Orozco RM, García-Jiménez C. Metabolic and hormonal remodeling of colorectal cancer cell signalling by diabetes. Endocr Relat Cancer 2021; 28:R191–R206

26. Babel I, Barderas R, Díaz-Uriarte R, Martínez-Torrecuadrada JL, Sánchez-Carbayo M, Casal JI. Identification of tumor-associated autoantigens for the diagnosis of colorectal cancer in serum using high density protein microarrays. Mol Cell Proteomics 2009;8:2382–2395

27. Babel I, Barderas R, Diaz-Uriarte R, et al. Identification of MST1/STK4 and SULF1 proteins as autoantibody targets for the diagnosis of colorectal cancer by using phage microarrays. Mol Cell Proteomics 2011;10:M110.001784

28. Barderas R, Babel I, Díaz-Uriarte R, et al. An optimized predictor panel for colorectal cancer diagnosis based on the combination of tumor-associated antigens obtained from protein and phage microarrays. J Proteomics 2012; 75:4647–4655

29. Morikawa K, Walker SM, Nakajima M, Pathak S, Jessup JM, Fidler IJ. Influence of organ environment on the growth, selection, and metastasis of human colon carcinoma cells in nude mice. Cancer Res 1988;48:6863–6871

30. Morikawa K, Walker SM, Jessup JM, Fidler IJ. In vivo selection of highly metastatic cells from surgical specimens of different primary human colon carcinomas implanted into nude mice. Cancer Res 1988;48:1943–1948

31. Brennan TV, Lin L, Huang X, Yang Y. Generation of luciferase-expressing tumor cell lines. Bio Protoc 2018;8:e2817

32. Garranzo-Asensio M, Guzmán-Aránguez A, Povedano E, et al. Multiplexed monitoring of a novel autoantibody diagnostic signature of colorectal cancer using HaloTag technology-based electrochemical immunosensing platform. Theranostics 2020;10:3022–3034

33. Garranzo-Asensio M, Guzman-Aranguez A, Povés C, et al. Toward liquid biopsy: determination of the humoral immune response in cancer patients

using HaloTag fusion protein-modified electrochemical bioplatforms. Anal Chem 2016;88:12339–12345

34. Garranzo-Asensio M, San Segundo-Acosta P, Povés C, et al. Identification of tumor-associated antigens with diagnostic ability of colorectal cancer by in-depth immunomic and seroproteomic analysis. J Proteomics 2020;214:103635

35. Barderas R, Shochat S, Timmerman P, et al. Designing antibodies for the inhibition of gastrin activity in tumoral cell lines. Int J Cancer 2008; 122:2351–2359

36. Garranzo-Asensio M, Guzmán-Aránguez A, Povés C, et al. The specific seroreactivity to ΔNp73 isoforms shows higher diagnostic ability in colorectal cancer patients than the canonical p73 protein. Sci Rep 2019;9:13547

37. Peláez-García A, Barderas R, Torres S, et al. FGFR4 role in epithelial-mesenchymal transition and its therapeutic value in colorectal cancer. PLoS One 2013;8:e63695

38. R Core Team. *R: A Language and Environment for Statistical Computing*. Vienna, Austria, R Foundation for Statistical Computing, 2015

39. Notterman DA, Alon U, Sierk AJ, Levine AJ. Transcriptional gene expression profiles of colorectal adenoma, adenocarcinoma, and normal tissue examined by oligonucleotide arrays. Cancer Res 2001;61:3124–3130

40. Kurashina K, Yamashita Y, Ueno T, et al. Chromosome copy number analysis in screening for prognosis-related genomic regions in colorectal carcinoma. Cancer Sci 2008;99:1835–1840

41. Anderson KS, LaBaer J. The sentinel within: exploiting the immune system for cancer biomarkers. J Proteome Res 2005;4:1123–1133

42. Casal JI, Barderas R. Identification of cancer autoantigens in serum: toward diagnostic/prognostic testing? Mol Diagn Ther 2010;14:149–154

43. Du Y, Grandis JR. Receptor-type protein tyrosine phosphatases in cancer. Chin J Cancer 2015;34:61–69

44. Suh S, Kim KW. Diabetes and cancer: is diabetes causally related to cancer? Diabetes Metab J 2011;35:193–198

45. Cannata D, Fierz Y, Vijayakumar A, LeRoith D. Type 2 diabetes and cancer: what is the connection? Mt Sinai J Med 2010;77:197–213

46. Stemmler MP, Eccles RL, Brabletz S, Brabletz T. Non-redundant functions of EMT transcription factors. Nat Cell Biol 2019;21:102–112

47. Nieto MA, Cano A. The epithelial-mesenchymal transition under control: global programs to regulate epithelial plasticity. Semin Cancer Biol 2012;22: 361–368

48. Nieto MA, Huang RY, Jackson RA, Thiery JP. Emt: 2016. Cell 2016; 166:21–45

49. Puisieux A, Brabletz T, Caramel J. Oncogenic roles of EMT-inducing transcription factors. Nat Cell Biol 2014;16:488–494

50. Ganesan R, Mallets E, Gomez-Cambronero J. The transcription factors Slug (SNAI2) and Snail (SNAI1) regulate phospholipase D (PLD) promoter in opposite ways towards cancer cell invasion. Mol Oncol 2016;10:663–676

AUTHOR QUERIES

AUTHOR PLEASE ANSWER ALL QUERIES

Q1: To ensure correct PubMed indexing for all authors, please highlight the surname for each author in the author group. If the surname includes multiple parts, ensure that all parts are highlighted.

Q2: In affiliation 4, please expand "CBS" in the Department name. Also, note that "University Rey Juan Carlos" was changed to "Rey Juan Carlos University" in affiliation 4 and in affiliation 7, please note that "Majadahonda" was added to "Hospital Universitario Puerta de Hierro" after fact-checking. Also, please expand UFIEC in affiliation 2 if it is part of the official name of the department or institution.

Q3: Please check that the conflict of interest information for each author is presented in full in the Duality of Interest section.

Q4: Correct expansion given for ROI (region of interest) in Figure 6?